ELSEVIER

Journal of Photochemistry and Photobiology A: Chemistry 113 (1998) 203–212

Journal of Photochemistry and Photobiology A:Chemistry

Fluorescence emission in fluid solution and supersonic jet of symmetrical bisbenzenes incorporating a three membered flexible chain

Françoise Lahmani [a,*], Anne Zehnacker [a], Jean-Pierre Desvergne [b,1], Henri Bouas-Laurent [b], Michel Colomes [b], Anke Krüger [b]

[a] *Laboratoire de Photophysique Moléculaire, CNRS UPR 3361, Bât. 213, Université de Paris Sud, Orsay 91405 Cedex, France*

[b] *Laboratoire de Photophysique et Photochimie Moléculaire, CNRS URA 348, Université Bordeaux 1, Talence 33405 Cedex, France*

Received 7 July 1997; received in revised form 9 December 1997; accepted 12 December 1997

Abstract

Intramolecular excimer formation in symmetrical bichromophore compounds consisting of two benzene, anisole, and 2,6-dimethylbenzene groups connected by a highly flexible O–CH_2–O chain has been evidenced from steady state and time resolved fluorescence studies. The thermodynamic and kinetic parameters have been determined in methanol and for one of them in methylcyclohexane as a function of temperature. While the activation energy for the conformational change required for excimer formation is similar for both solvents, the preexponential factors deduced from Arrhenius plots appear to be larger in methanol than in methylcyclohexane. The parallel investigation of fluorescence excitation and dispersed emission spectra of bis-*p*-methoxy-phenoxymethane in supersonic expansion has shown that two conformers coexist in the jet and that the intrinsic barrier for excimer formation in the isolated molecule is larger than 2.3 kcal mol^{-1}.

Keywords: Fluorescence emission; Symmetrical bisbenzenes; Intramolecular excimer formation

1. Introduction

Fluorescing excimers have been shown to play a major role in the mechanism of inter and intramolecular photocycloaddition [1–3] and to be an invaluable tool in the study of molecular dynamics in polymers [4–6] or molecular assemblies [7,8]. Thus, the polymethylene chains have been extensively investigated in many α,ω-bisarylalkanes (Ar–$(CH_2)_n$–Ar) [9–14]. From a study of α,ω-bisphenylalkanes, Hirayama [15] concluded that the $(CH_2)_3$ spacer was the most favorable to observe the benzene excimer: these results, known as Hirayama's rule, suggest that three membered links are the most efficient to generate excimer type complexes. In such systems, linked by a polymethylene chain, excimer formation has also been shown to depend not only on the spacer geometry but also on its conformational mobility: as the bichromophores are rather floppy molecules, several conformations are expected to coexist at room temperature. For example, time resolved fluorescence measurements on di(naphthyl)propane in solution have been rationalized in terms of a kinetic scheme involving two ground state conformations [16]. In addition, it has been shown by jet experiments that four isomers of 1,3-diphenylpropane are cooled down in the jet and that the barrier for intramolecular excimer formation is strongly dependent on the chain geometry [17] and is significantly lower for the conformation tentatively assigned to the gauche–gauche isomer.

For bis-α,ω-9-anthrylalkanes, Hirayama's rule does not apply, i.e., no excimer fluorescence has been detected for $n=3$, but the highest excimer emission intensity was observed for $n=5$ and 6 [10]. However, the trimethylene chain (–$(CH_2)_3$–) was found to be efficient for the photocycloisomerization [10]; an increase of the chain flexibility by using the CH_2–O–CH_2 link led to a higher photoclosure efficiency whereas the highest photoreactivity was observed for the '–O–CH_2–O' (denoted 'acetal') spacer [18,19]. For none of these three member spacers was an excimer emission detected [18,19]. This photoreactivity could compete with the excimer radiative deactivation. Less reactive bisaryls (such as phenyl, naphthyl, pyrenyl, etc.) obey Hirayama's rule. Therefore, it was anticipated to observe an excimer fluorescence for bisbenzenes when the two rings are connected together with the acetal link which was found to be so far the most flexible spacer for bisanthracenes. Indeed, in

* Corresponding author.

[1] Also corresponding author.

1010-6030/98/$19.00
PII S1010-6030(98)00199-3

contrast to its anthracene analog, the excimer of **2** has been characterized by its spectrum in methanol at room temperature [20].

In this paper, we present the results of a systematic investigation of the electronic absorption and emission spectroscopy of bisbenzenes **1–3** together with their reference monochromophoric derivatives **4–6**

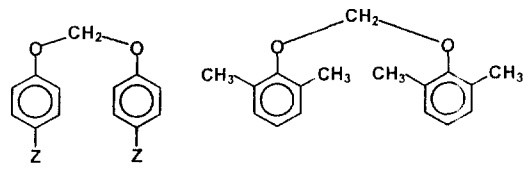

Z = H **1** **3**

Z = OCH_3 **2**

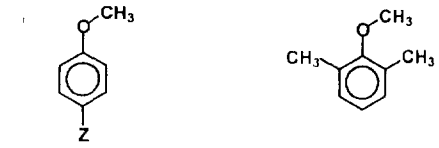

Z = H **4** **6**

Z = OCH_3 **5**

respectively, at different temperatures, in methanol and methylcyclohexane solutions, in order to determine the kinetic parameters associated with the monomers (locally excited species) and excimers reactivity (Scheme 1). These results are compared with those of an investigation of the **2–6** derivatives, using the supersonic jet technique.

The aim of the supersonic jet experiments is to compare the fluorescence properties of the isolated bichromophore with those in condensed fluid solutions. The excited state dynamics of jet-cooled bichromophores are expected to be strongly dependent on the ground state geometry of the spacer and on its flexibility. When the 0–0 band of the bichromophore is excited, no conformational relaxation can take place in the excited state. On the other hand, when exciting the system with some excess energy, intramolecular vibrational redistribution (IVR) takes place and may populate chain modes which permit conformational changes in the excited state and give rise to excimer formation under isolated conditions.

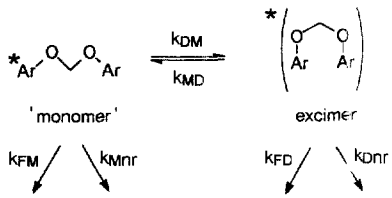

Scheme 1. k_{FM}, k_{FD}, fluorescence rate constants of 'monomer' and excimer emissions, k_{Mnr} and k_{Dnr} non-radiative deactivation rate constants for monomer and excimer, respectively.

We have recently studied, using the supersonic jet technique, the laser induced excitation and emission spectra of compound **1** and **3** [21]. While no evidence for excimer formation has been found for **1** in the gas phase, at least when excited with less than 1000 cm^{-1} excess energy, there is an indication of the formation of a weakly fluorescent excimer in the case of sterically hindered compound **3** close to the absorption threshold.

2. Experimental

2.1. Preparation of compounds 1–3

The bichromophore **2** was synthesized according to published procedures [21]. Bichromophore **1** was prepared using the Dehmlow method [22], the preparation of compound **3** has been described in a previous paper [20].

2.2. Solvents

Solvents of spectrometric grade were purchased commercially and used without further purification. Methanol [purchased from Solvants Documentation Synthèses (SDS)] was carefully distilled upon Mg turnings with a 1 m column prior to use. No fluorescent contaminants were detected upon excitation in the wavelength region of experimental interest.

2.3. Spectroscopic methods

UV spectra were recorded on a Hitachi U-3300 spectrometer, and fluorescence spectra with a Hitachi F-4500 instrument corrected for emission and excitation. The samples (concentration $\leq 10^{-5}$ M) were degassed by freeze–pump–thaw cycles on a high vacuum line and sealed under vacuum. The fluorescence quantum yields were determined on degassed samples by comparison with 1,4-dimethoxybenzene (ϕ_F: 0.21 cyclohexane) and anisole (ϕ_F: 0.29 cyclohexane) taking into account the refractive index influence for methanol [23].

The temperature dependent measurements (UV and fluorescence) were performed using a quartic cell, 1 cm optical pathlength, placed in a copper holder inside a quartz Dewar flushed by cold nitrogen gas; the temperature (± 0.5°C) monitored by a platinum sensor was adjusted by the nitrogen flow.

Fluorescence decay measurements were performed using the single-photon timing technique (Applied Photophysics). The decay parameters were determined by a nonlinear least squares deconvolution method, the DECAN (1.0) programme [24], kindly provided by F. De Schryver. The success of the fits was evaluated by reduced χ^2 (0.95–1.2), the randomly distributed weighted residuals, the autocorrelation function of weighted residuals and the Durbin–Watson parameters. The kinetic parameters were estimated to be determined with an accuracy of ca. 10%.

A biexponential decay obeys the following equation:

$$I_F(t)=A_1\exp(-\lambda_1 t)+A_2\exp(-\lambda_2 t) \quad (1)$$

As an example, the experimental data for the fluorescence decay of compound **2**, in CH_3OH (λ obs: 315 nm) were found to be the following:

Temperature	A_1	$1/\lambda_1$ (ns)	A_2	$1/\lambda_2$ (ns)	χ^2
62°C	1.81	0.45	0.017	7.5	1.12
20°C	1.58	0.59	0.045	7.9	1.11
−10°C	0.78	1.16	0.014	8.3	1.08
−43°C	0.76	1.9	0.006	9.0	1.02

Kinetic parameters (k_{DM}, k_{MD}, k_{FD}, k_D,..., see Scheme 1) were evaluated from the following equations based on the Birks model (fluorescence decay of a locally excited species *and* one excimer); then, the time evolution of the emission from the locally excited species $I_M(t)$ and from the excimer $I_D(t)$ can be expressed as follows [25]:

$$I_M(t)=k_{FM}(\lambda_2-X)/(\lambda_2-\lambda_1)(\exp(-\lambda_1 t)+A\exp(-\lambda_2 t)),$$

$$I_D(t)=k_{FD}k_{DM}/(\lambda_2-\lambda_1)(\exp(-\lambda_1 t)-\exp(-\lambda_2 t)),$$

where $\lambda_{1,2}=1/2\{(X+Y)\pm[(X-Y)^2+4k_{DM}k_{MD}]^{1/2}\}$;
$X=k_{DM}+k_M$ corresponds to the deactivation channels of the locally excited monomer; $Y=k_{MD}+k_D=\lambda_1+\lambda_2-X$ corresponds to the deactivation channels of the excimer state; $A=A_2/A_1=(X-\lambda_1)/(\lambda_2-X)$, X and Y can be expressed as a function of A, λ_1, λ_2 and thus deduced from the experimental data:

$$X=(A\lambda_2+\lambda_1)/(A+1)$$

$$Y=(A\lambda_1+\lambda_2)/(A+1)$$

$$k_{DM}=(A\lambda_2+\lambda_1-k_M(A+1))/(A+1)$$

$$k_D=\{(A\lambda_1+\lambda_2)/(A+1)\}-k_{MD};$$

$$k_{MD}=(X-\lambda_1)(\lambda_2-X)/k_{DM}$$

$$k_{MD}=(k_M+k_{DM}-\lambda_1)\times\{(\lambda_2-(k_M+k_{DM})\}/k_{DM}$$

$$k_{FM}=\phi_{FM}/\tau_M;\ k_M=1/\tau_M$$

$$k_{FD}=\phi_{FD}\times k_{FM}(k_D+k_{MD})/\phi_{FM}\times k_{DM}$$

2.4. Jet experiments

The experimental setup has been described [21]. The free supersonic expansion is obtained by expanding the carrier gas (Helium at 2 atm backing pressure) saturated with the vapor of the compounds under study (from heated samples) through a 200-μm pinhole into a vacuum chamber. The chromophores are excited in their first electronic transition 5 mm downstream by a frequency-doubled (BBO) dye laser (Coumarin 540A or Rhodamine 590), pumped by the third or second harmonic of a YAG Laser (BM Industrie or Quantel). Fluorescence was observed at right angle, either through filters (WG 285, WG 320) or dispersed by a monochromator (60 cm length Jobin–Yvon) and detected by a photomultiplier (Hamamatsu R2059). The signal from the photomultiplier is averaged and processed through gated detection electronics connected to a personal microcomputer.

3. Results

3.1. Fluid solution studies

The spectra were recorded in methanol (MeOH) and methylcyclohexane (MCH) as a function of temperature. While the same behavior is qualitatively observed in both solvents, the fluorescence intensity and decay kinetics appear to be sensitive to the nature of the solvent. Most results are given for MeOH; some striking features in MCH are commented upon when necessary.

3.1.1. UV absorption spectra

Compound **2** has previously [20] been found to display an hypsochromic shift ($\Delta\nu\approx 510\ cm^{-1}$) and an hypochromic effect, in comparison with the reference molecule **5**; the same is true for **1** ($\Delta\nu\approx 470\ cm^{-1}$) as compared with **4** (Fig. 1).

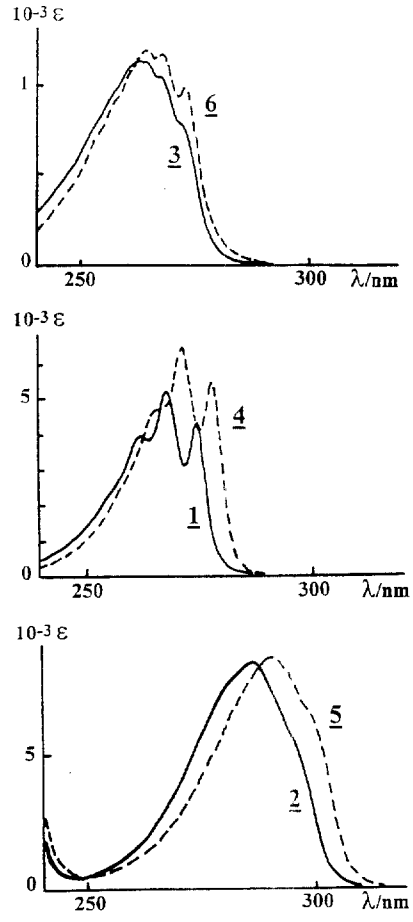

Fig. 1. UV absorption spectra of bichromophores **1–3** and reference molecules **4–6** (2 ε) in CH_3OH at *RT* (conc. $\approx 10^{-4}$). A clear hypsochromic shift is observed between the bichromophores and the reference compounds. $\Delta\nu_{max}$ (taken at the intensity maximum): **1–4** = 470 cm^{-1}; **2–5** = 510 cm^{-1}; **3–6** ≈ 260 cm^{-1}.

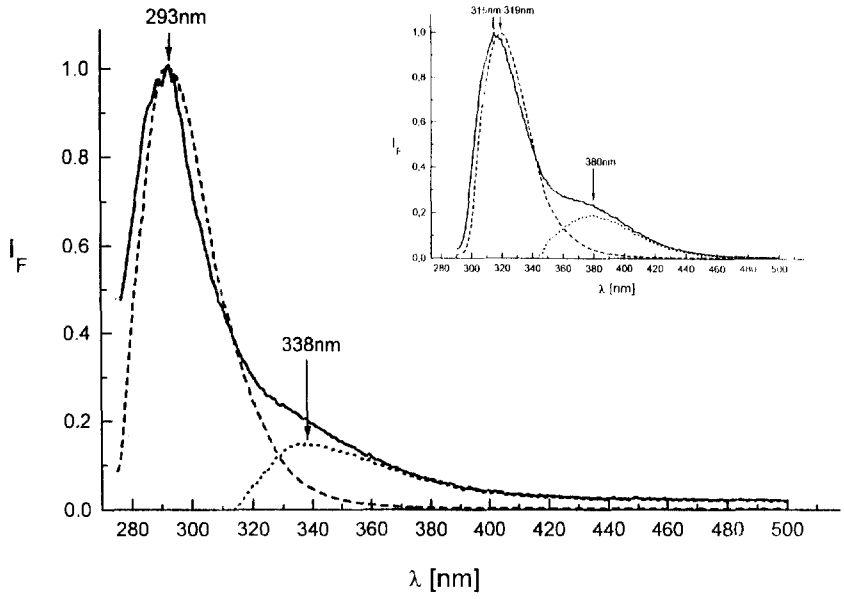

Fig. 2. Corrected fluorescence emission spectra (normalized) in CH_3OH of compounds **1** (——) (bichromophore) and **4** (reference) (- - -) at 20°C; conc. $\leq 10^{-5}$ M, λ_{exc}: 270 nm. The excimer spectrum (· · ·) was deduced by the difference between **1** and **4**. Similar spectra were obtained for **2** and **5** (shown in insert) as well as **3** and **6**.

The hypsochromic shift in the bichromophores is presumably ascribable to a decrease in conjugation between the oxygen lone-pairs and the aromatic π-clouds due to an enhanced steric hindrance between the groups in the bichromophores; the hypochromic effect suggests some degree of superimposition between the benzene rings [26–28]. Qualitatively, similar variations can be observed between compound **3** and the reference molecule **6** (Fig. 1) but attenuated ($\Delta\nu \approx 260$ cm^{-1}) because, in the latter, the methoxy group interacts with the two methyl groups in positions 2 and 6 adopting a nonplanar conformation more similar to that of $O-CH_2$ in the bichromophore [21]. Thus, the three bisbenzenes incorporating an acetal link display a consistent picture. The better the conjugation, the stronger the red shift (**2** > **1** > **3**) (Fig. 1).

3.1.2. Fluorescence emission spectra

Although the fluorescence emission spectra (conc. $\leq 10^{-5}$ M) of **1–3** resemble those of **4–6**, they present some changes in the long wavelength region (Fig. 2). Subtraction of spectrum of **4–6** from that of **1–3** reveals a new, weak and non structured band assigned to an intramolecular excimer emission (intermolecular process is discarded as no concentration effect has been noted). This assignment is borne out by the excitation spectra which match the absorption spectra and are independent on the wavelength of observation; they prove the common origin of the two emissions. Finally, the existence of the second component of the fluorescence emission was fully confirmed by the fluorescence decay profiles of **1–3** which are best fitted by a biexponential function (vide infra).

3.1.3. Stevens–Ban plots

When the solutions were cooled (from 293 K down to ca. 200 K) an increase of the total fluorescence emission was observed (except for **3** for which ϕ_F remains approximately constant and <0.10) accompanied with a change of the relative contribution of excimer and 'monomer' components (Fig. 3). The logarithms of the ratio of fluorescence quantum yield in excimer and 'monomer' part vs. $1/T$ gave the so-called Stevens–Ban plots [29] (Fig. 4). Provided there is an interconversion between 'monomer' and excimer species, it is possible to evaluate the activation energy (ΔE) for excimer formation and its enthalpy of stabilization (ΔH) from the tangents at the 'Stevens–Ban' curve in the low- and high-temperature regions, respectively (however, ΔE for **3** and ΔH for **2** could not be determined due to the scarcity of points

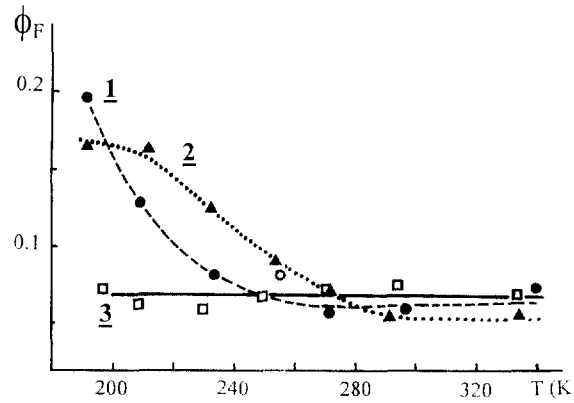

Fig. 3. Temperature dependence of total fluorescence quantum yields (ϕ_F) of compounds **1–3** in degassed CH_3OH (**1**) (- - -), (**2**) (· · ·), (**3**) (— — —). In the same temperature interval the reference compounds quantum yields (ϕ_M) were found to display the following values at 340 K and 200 K, respectively. **4**: 0.18–0.36; **5**: 0.12–0.24; **6**: 0.12–0.23.

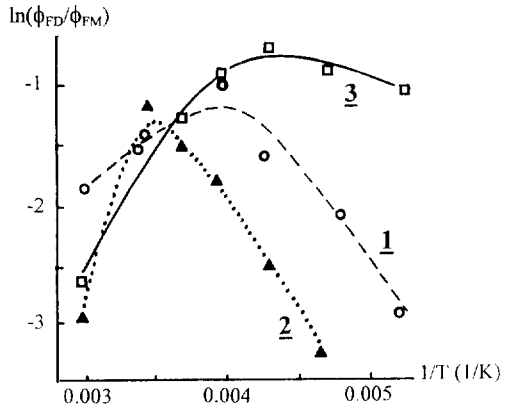

Fig. 4. Plots of the logarithm of the ratio of fluorescence quantum yields in excimer and 'monomer' vs. $1/T$ in degassed CH_3OH (Stevens–Ban plots) for compounds **1–3**; for ΔE and ΔH data, see Table 1.

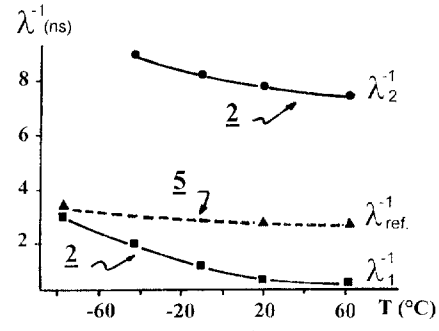

Fig. 5. Fluorescence decay lifetimes ($1/\lambda_1$) of compounds **2** (——) and **5** (- - -) in degassed CH_3OH recorded in the monomer region (≈ 300 nm) vs. temperature. At low temperature, λ_1^{-1} and $\lambda_{ref.}^{-1}$ (ref.) converge to the same value. Spectra of the same type have been recorded for (**1** and **4**) and (**3** and **6**).

in the relevant regions the measurement domain being limited by the boiling [338 K] and freezing [179 K] points of methanol). Nevertheless, these values have to be taken with caution because of the approximations related to the method (among the usual hypotheses, the radiative rate constants k_{FM} and k_{FD} for 'monomer' and excimer, respectively, are considered as independent on temperature) they are in the same order of magnitude as those determined from fluorescence decays analysis (Table 1) and will be discussed in a following paragraph.

3.1.4. Transient kinetic analysis

In contrast with the reference compounds **4–6**, which display, at all temperatures, a single exponential fluorescence emission decay, the emission profile of bichromophores **1–3** were best fitted with a linear combination of two exponentials whatever the observation wavelength considered. The study of the decays vs. temperature was only performed in the 'monomer' region ($I_M(t)$) because the excimer emission was not intense enough to be measured under our experimental conditions; however, the few experiments carried out on the excimer region at room temperature gave kinetic parameters similar to those obtained on the 'monomer' part; then the decays were adjusted with a difference of two exponentials on the excimer part whereas a sum of two exponentials is necessary for the monomer region (Scheme 1); these results indicate that the Birks kinetic scheme [25] applies for compounds **1–3**

The fluorescence lifetimes, as observed with the fluorescence emission quantum yields, are temperature dependent (Fig. 5). Indeed, when temperature is decreasing, a monotonous increase of the lifetime of **4–6** is recorded. Besides, the two decay parameters found for **1–3** are simultaneous growing with cooling the solution; the smallest kinetic parameter $1/\lambda_1$ and the lifetime of **4–6** have a tendency to converge at low temperature; concomitantly the ratio of the preexponential factors A_2/A_1 is strongly reduced.

Table 1
Fluorescence quantum yields (ϕ_F), thermodynamic and kinetic parameters for compounds **1–3** and **4–6** in methanol at 20°C

Compound	ϕ_F	λ^{-1} (ns)	k_{DM} (10^9 s^{-1})	k_{MD} (10^9 s^{-1})	ΔE (kcal/mol)	$-\Delta H$ (kcal/mol)	Excimer λmax (nm) ($\Delta\nu$ cm^{-1})	ΔU_i (kcal/mol)
1	0.06	0.26 and 6.2 ($A_2/A_1 = 0.217$)	3.1	0.65	(2.9)[a], 4.4[b]	(1.7)[a], 3.1[b]	346 (4,550)	9.9
4	0.22	7.5						
3	0.08	0.18 and 8.6 ($A_2/A_1 = 0.109$)	4.8	0.54	3.2[b]	(3.5)[a], 3.2[b]	347 (5,200)	11.7
6	0.16	5.7						
2	0.055	0.59 and 7.9 ($A_2/A_1 = 0.028$)	1.3	≈0.05	(4.0)[a], 4.7[b]		380 (5,430)	–
5	0.16	2.7						

ΔE and ΔH activation energy and enthalpy for excimer formation. λ^{-1} was determined by single photon timing by analyzing the 'monomer' fluorescence decay

ΔU_i intramolecular repulsive potential in the ground state between two phenyls after radiative deactivation of the excimer.

The accuracy of rate and thermodynamic constants was estimated to be ca. 15%.

[a]From Stevens–Ban plots.

[b]From single photon timing data.

[c]Not calculated due to the very low and not accurate value of k_{MD}. A_2 and A_1 are the preexponential factors in Eq. (1).

These data (k_{DM}, k_{MD}, ΔE) compare well with those for 1,3-bisphenylpropane [5], dibenzylether [5], 1,3-di-α-naphthylpropane [13,23], di(α-naphthylmethyl)ether [5], 1,3-di-β-naphthylpropane [13] and bis(*p*-diphenylmethyl)ether [11]. $\Delta\nu = \nu_0$ (onset of the fluorescence emission) $- \nu_{max}$ (excimer max emission wavenumber).

For **1**, **4**, **3**, **6**: $\lambda_{exc} = 270$ nm and $\lambda_{obs} = 300$ nm; for **2**, **5**: $\lambda_{excit} = 289$ nm and $\lambda_{obs} = 315$ nm.

This shows that the reference molecules chosen (**4–6**) are pretty good models for the locally excited states ('monomers') despite the slight difference with the bichromophores shown at the onset of the fluorescence spectra (λ_0, see Fig. 2). Therefore, for the calculation of the rate constants of Scheme 1, k_{FM} was obtained from the quantum yields ϕ_{FM} and lifetimes τ_M of the reference compounds **4–6**. Using these values and the transient kinetics data, the rate constants were calculated (see Section 2). Some of these, particularly k_{DM} (excimer formation) and k_{MD} (excimer dissociation) (at room temperature), are collected in Table 1. The kinetic analysis was conducted in the temperature interval $-80°$ to $+60°C$ in order to derive the activation energies for excimer formation (ΔE) and dissociation ($|\Delta H| + \Delta E$) (see Fig. 6) by plotting ln (k_{DM}) and ln (k_{MD}) vs. $1/T$, respectively (Fig. 7a and Table 1). Similar experiments were performed in MCH for compound **2** (see plotted data in Fig. 7b).

3.1.5. Repulsive potential ΔU_r

The excimer emission is known to occur at longer wavelength (λ_{max}) than that of the locally excited emission (λ_0: onset of the fluorescence spectra [see Fig. 2]). The Stokes shift $\Delta\nu = \nu_0 - \nu_{max}$ has often been assumed to be an approximate measure of the excimer stabilization. But, when one considers an energy profile for excimer formation (Fig. 6), it appears that this value also includes the ground state repulsive potential

$$h\Delta\nu = |\Delta H| + \Delta U_r$$

The determination of ΔH for bichromophore **1** and **3** (≈ -3 kcal mol^{-1}) allows the calculation of the repulsive energy ΔU_r, i.e., ca. 10 kcal mol^{-1} (**1**) and 11.5 kcal mol^{-1} (**3**) (Table 1).

3.2. Isolated molecules in supersonic jet

The spectroscopic properties of jet cooled bichromophores **1** and **3** have already been reported [20]. Therefore, we concentrate here to the laser induced fluorescence spectroscopic study of compound **2**. Solution spectra have shown that this bichromophore gives rise to the largest excimer intensity and is thus more suitable to evidence the excimer formation under jet cooled conditions.

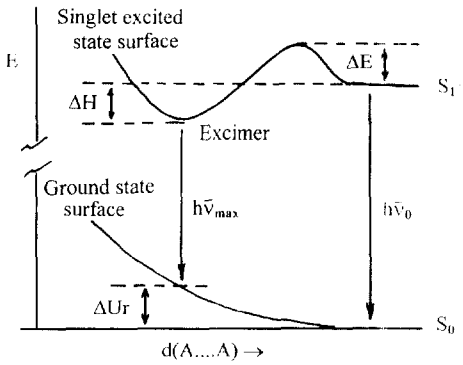

Fig. 6. Energy profile for excimer formation between two aromatic (A) rings situated at the mutual distance d(A...A). ΔE and ΔH are the activation energy and stabilization enthalpy, respectively. ΔU_r represents the ground state repulsive potential at the excimer equilibrium distance. $h\nu_0 = |\Delta H| + h\nu_{max} + \Delta U_r$.

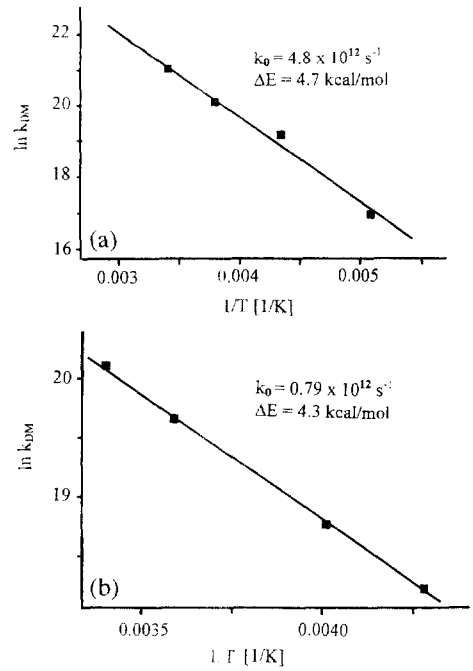

Fig. 7. Plots of ln k_{DM} vs. $1/T$ according to the equation ln $k_{DM} = k_0$ exp ($-\Delta E/RT$); k_{DM} is the rate of intramolecular excimer formation for compound **2**; (a) in MeOH, $r = 0.9937$ (b) in MCH, $r = 0.9991$.

3.2.1. Fluorescence excitation spectra

The fluorescence excitation spectrum of 1-4-dimethoxybenzene **5** has been recorded for the sake of comparison and is the same as that published by Yamamoto et al. [30]. It displays two intense features located at 33,631 and 33,851 cm^{-1}, attributed to the 0–0 transition of the *trans* and *cis* rotational isomers, respectively. The main vibrational levels in the S_1 state of the *cis* and *trans* isomers are reported in Table 2.

The fluorescence intensity of the bichromophore is weak when compared to the monomer, which shows that an efficient nonradiative process takes place in the bichromophore.

Table 2
Main vibrational frequencies (cm^{-1}) observed in the reference compound **5** and the bichromophore **2**

Cis isomer (origin at 33,851 cm^{-1})		*Trans* isomer (origin at 33,631 cm^{-1})		Bichromophore (origin at 34,245 cm^{-1})	
S_0	S_1	S_0	S_1	S_0	S_1
–	316, 370	405	386		372
528	505	551	–	530	510
824	808	821	811	824	805
1330	1300	1275	1298	1330	

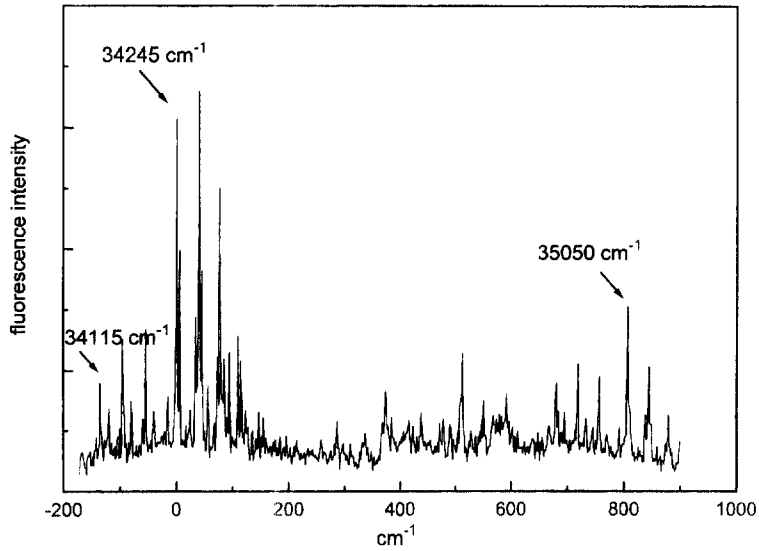

Fig. 8. Fluorescence excitation spectrum of the bichromophore 2 in a supersonic expansion obtained by collecting the total emission. (Temperature of the reservoir sample, $T = 110°C$.) The frequency scale is relative to the strongest 0–0 transition at 34,245 cm^{-1}. The arrows indicate the bands pumped for dispersed emission spectra of Fig. 9.

This result is corroborated by decay measurements which shows that the fluorescence lifetime of **2** is contained in the laser pulse (<8 ns). The excitation spectrum (Fig. 8) displays a series of bands centered around 34,200 cm^{-1}, i.e., blue shifted relative to the monomer. It is composed of two systems of bands whose origins are located at 34,115 and 34,245 cm^{-1}, respectively. In the case of **1** only one system was observed at origin and the presence of two systems in **2** may be correlated with the existence of different isomers corresponding to different orientation of the terminal OCH_3 as observed in the monomer **5**. Under this assumption, the 0–0 bands of the two forms of **2** are blue shifted by 484 and 394 cm^{-1} with respect to the *trans* and *cis* forms of the monomer **5**. It should be noted besides that the energy gap between both isomers is reduced from 220 cm^{-1} in **5** to 130 cm^{-1} in **2**. The strongest band at 34,245 cm^{-1} is followed by a progression of 40 cm^{-1} centered on the 0–0 transition. Each band of the progression is composed of a doublet split by less than 5 cm^{-1}. The same 40 cm^{-1} progression is observed from the 34,115 cm^{-1} origin. This low-frequency mode is close to those observed in bisphenoxymethane **1** (42 and 48 cm^{-1}) and may be assigned to a torsion of the acetal chain. Another progression of weaker intensity built on the same low-frequency mode has its origin at 34,128 cm^{-1}.

Higher vibronic levels displaying a similar low frequency structure appear with significant intensity at 510 and 805 cm^{-1} from the most intense origin at 34,245 cm^{-1}. These modes correspond to those observed in *cis*-1,4-dimethoxybenzene at 505 and 808 cm^{-1}. Similarly, a series of weaker bands is obtained to the red of the intense 805 cm^{-1} features reproducing the structure observed at origin. Other weaker bands at 290 and 370 cm^{-1} from the strongest origin are more difficult to assign to either forms of **2**.

3.2.2. Dispersed emission spectra

The emission spectrum resulting from the excitation of the bichromophore **2** at 34,115 and 34,245 cm^{-1} is presented on Fig. 9. Both emission spectra display the same vibrational

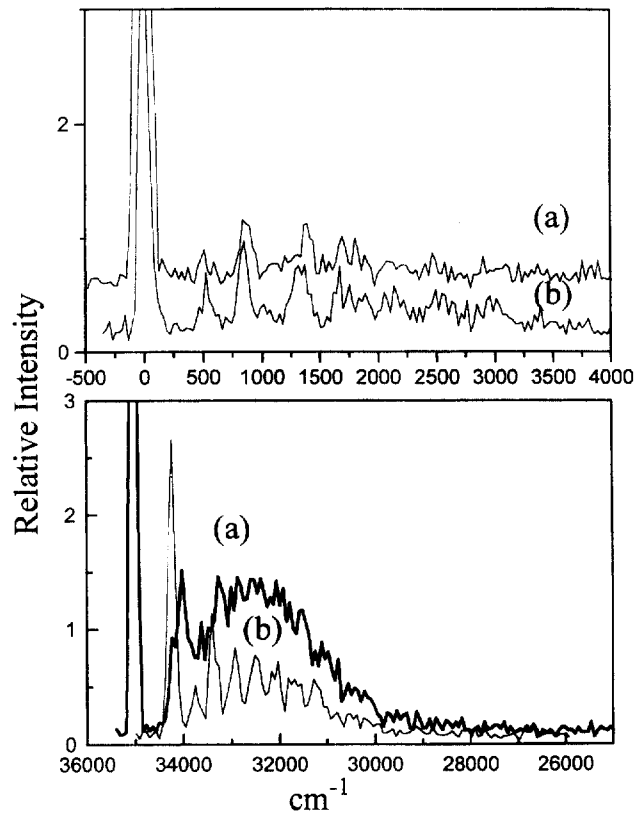

Fig. 9. Dispersed fluorescence spectra of the bichromophore **2**: upper part: 0^0 level excitation at: (a) 34,115 cm^{-1}, (b) 34,245 cm^{-1}. Lower part: (a) excitation of the 805 cm^{-1} vibronic level at 35 050 cm^{-1}, (b) 0^0 excitation at 34,245 cm^{-1} recorded under the same conditions shown for comparison.

structure with main bands at 530, 825, and 1330 cm^{-1}. Similar frequencies are observed for the *cis* isomer of the monomer (see Table 2). It is, however, difficult to conclude from this comparison that the excited subunit in the bichromophore has the *cis* conformation. An out-of-plane gg geometry has been calculated for bisphenoxybenzene **1** [20]. The substitution with OCH_3 groups in *para* position from the chain is not expected to modify this conformation in **2**. In a nonplanar geometry, the distinction between *cis* and *trans* forms is not relevant.

The dispersed fluorescence obtained by pumping the main 805 cm^{-1} feature shown on Fig. 9 is broad and slightly red shifted with respect to that originating from the 0^0 level. This behavior is characteristic of intramolecular vibrational redistribution (IVR). There is no indication of a tail extending toward the red which may reveal the formation of an intramolecular excimer as observed in solution.

4. Discussion

4.1. Solution experiments

The steady state fluorescence together with the detailed kinetic analysis of the decays of compounds **1**, **2**, **3** show unambiguously that the bisbenzene molecules linked with a $O–CH_2–O$ chain (acetal linkage) give rise to intramolecular excimer formation. The excimer formation process in bichromophoric systems is supposed to be determined by two factors. The first one concerns the resonance interaction energy gained in the parallel configuration of the aromatic rings which stabilizes the excited complex in a potential energy minimum from which a radiative process toward the repulsive part of the ground state can take place. The second one deals with the rotational motion of the chain needed to overcome the potential energy barrier and reach the best overlapping arrangement of the aromatic rings (Fig. 6). It is the rate determining step. As mentioned in Section 1, extensive studies have been performed on the mechanism of excimer formation on bichromophores including large polyaromatic moieties (naphthalene, anthracene, biphenyl, pyrene [9–14]) linked by a polymethylene chain. However, although a dual fluorescence emission has been observed in related bisbenzenes such as $C_6H_5–X–C_6H_5$, where $X=(CH_2)_3$ [15]; $CH_2–O–CH_2$ [31] $CH_2–NHR–CH_2$ [32,33] or O–P(O) OH–O [34]; there is a dearth of data on the kinetics and thermodynamics of excimer formation: this is presumably connected to their much weaker and less shifted excimer fluorescence indicating smaller resonance stabilisation energy as expected from more limited overlap of the π system and low transition moments of the interacting excited states.

The present study brings quantitative new data on the intramolecular excimer energetics (ΔE and ΔH values) and dynamics (rate of formation k_{DM} and of dissociation k_{MD}) in the case of the flexible acetal linkage which may be compared with available results on similar systems. The ΔE values are in the same range as those found for 1,3-bis-diphenylpropane (3.9 kcal mol^{-1}) and dibenzylether (3.7 kcal. mol^{-1}) in ethanol [5], as well as several other similar bisarenes [35]. The stabilization enthalpies (ΔH) although weak are not very different from those of other bisarenes [35]. The ΔU_r values are in the range of those found for other intramolecular excimer systems bis(1-pyrenyl)propane (ca. 14 kcal) in *n*-heptane [12] and a mixed 9-anthryl-1-pyrenyl mixed excimer (ca. 11.5 kcal in MeOH [36]). However, they are higher than those reported for intermolecular excimers of benzene derivatives: ΔU_r/kcal mol^{-1}: pure toluene (7.0), pure mesitylene (8.0). The interesting feature is that although both excimers **1** and **3** have the same ΔH values, the ground state repulsion energy of **3** is higher, presumably because of the steric hindrance of the methyl derivatives in positions 2 and 6.

Regarding the kinetic data, one salient feature is the high values of k_{DM} (1.3 to 4.8 $\times 10^9$ s^{-1}) which are clearly larger than those of other related bisarenes (2 to 7×10^8 s^{-1}), in line with a higher flexibility of the acetal link than those of other three member spacers. AM1 calculations on the conformations of compounds **1** and **3** have been reported in the previous article. It has been shown that the $O–CH_2–O$ link in **1** can take either a gg or a tg conformation with similar heats of formation ($\Delta H_{gg} = -26.5$ kcal mol^{-1}, $\Delta H_{tg} = -25.4$ kcal mol^{-1}) while the tg configuration is the most stable in compound **3**. A single ground state species of **1** is stabilized in the conditions of the supersonic jet as deduced from the laser induced fluorescence study of **1** and has been attributed to the gg conformation. However, the two different conformations of the bichromophores can be in equilibrium in solution at room temperature. The coexistence of multiple conformers would lead to deviation of the simple Birks kinetics and manifests itself by multiexponential behavior in the decays [12]. This deviation is not observed experimentally. In addition, it is interesting to note that the fastest rate is observed for the 2,6-dimethyl derivative **3** which should have a *trans* gauche ground state geometry more conducive to that of the excimer.

The reciprocal lifetimes k_D of the intramolecular excimers ($1/\tau_D = k_D = k_{FD} + k_{Dnr}$) were found in the range 1.1 to 1.7×10^8 s^{-1} and compare well to that given for benzene itself [25] in hexane ($k_D = 0.83\times10^8$ s^{-1}).

Another interesting result which should be stressed is the solvent effect observed in excimer formation efficiency. Steady state fluorescence at room temperature shows that the intensity of the intramolecular excimer fluorescence is larger by a factor of 2–3 in methanol than in methylcyclohexane. Both the temperature dependence of the monomer to excimer fluorescence ratio and time constants deduced from monomer decays indicate that the thermodynamic values of ΔE and ΔH are only slightly modified by the solvent. Thus, the static change of the potential energy surface which could have resulted from specific solvent solute interactions (for example, polarity effect) is not involved in the observed phenomenon. This can be understood if one considers that the charge

transfer contribution should not play a significant role in bisbenzene excimer stabilisation.

The analysis of the fluorescence decays as a function of temperature shows that the preexponential factors of the Arrhenius equation for the barrier crossing are responsible for the different behavior obtained in MeOH vs. MCH. The preexponential factors decrease from 4.8×10^{12} in MeOH to 0.8×10^{12} in MCH (Fig. 7). The process of excimer formation has been largely used in the past to probe the role of the solvent on the dynamics of conformational changes through a barrier in flexible molecules in the frame of the theoretical treatment developed by Kramers [36]. This approach involves the description of solute solvent frictional coupling which is directly related to the solvent viscosity η and appears in the preexponential factor of the Arrhenius equation. In the high friction limit, the preexponential factor is shown to be proportional to η^{-1}. Under the assumption that the temperature dependence of the viscosity can be written as:

$$\eta^{-1}=\eta_0^{-1}\exp(-E_\eta/RT)$$

the η_0^{-1} factors and E_η values can be calculated from the tables on viscosity temperature relationship [37]. $\eta_0^{-1}=23.5$ cP^{-1} and 100 cP^{-1} and $E_\eta=1.7$ and 2.4 kcal mol^{-1} for MCH and MeOH, respectively. From this estimation it can be deduced that the preexponential factor should be larger by a factor of 4.25 in MeOH relative to MCH. Although the high friction limit may be too rough an approximation for the solvents used here and a more systematic investigation of the role of the solvent viscosity should be required to confirm these results, this estimation compares satisfactorily with the experimental value of 6.

4.2 *Jet experiments, comparison with solutions*

As observed in solution, the origin of the S_0–S_1 transition in isolated compound **2** exhibits an hypsochromic shift relative to the monomer **5** ($\Delta\nu=\sim400$ cm^{-1}). This effect has been previously observed in compound **1** and has been related to the out-of-plane gg geometry of the O–CH_2–O chain on the basis of quantum chemistry calculations. One can assume that the same geometry of the chain is maintained in **2**. However, while the excitation spectrum of **1** is relatively simple in the 0–0 transition region (a single isomer, two low frequency modes at 42 and 48 cm^{-1}), the spectrum of **2** appears much more complicated. As discussed before, the two strongest transitions at 34,115 and 34.245 cm^{-1} can be assigned to two rotamers which may correspond to different orientations of the OCH_3 substituent in *para* position from the link by analogy with reference compound **5**. However, one cannot exclude the presence of isomers due to different conformations of the O–CH_2–O chain and the multiplet structure of the bands may indicate a more complex behavior. It is to be noted that four different conformers have been evidenced recently in the case of 1-3-diphenylpropane in supersonic jet [17].

The second point is relative to the absence of excimer formation in **2** at least for an excess energy of 2.3 kcal mol^{-1}. Unfortunately, the weakness of the fluorescence signal prevents the exploring of the higher energy region. The barrier determined in solution is 4.7 kcal mol^{-1} and 4.3 kcal mol^{-1} in MeOH and MCH, respectively. By considering the viscosity term in the activation energy as previously discussed (2.4 and 1.7 kcal mol^{-1} for MeOH and MCH), one may predict an intrinsic energy barrier of about 2.6 kcal mol^{-1}. The lack of excimer fluorescence in jet conditions for similar excess energy may be related to a conformation dependence effect as recently reported in the case of 1-3 diphenyl propane [17]. In the isolated system, the excess vibrational energy in the optically prepared ring mode is subject to rapid internal redistribution (IVR) which populates numerous isoenergetic levels. Some of them may give way to the reactive torsional motions and subsequently to the excimer while the other nonreactive modes are responsible for the monomer like emission. For the gg conformation which has been calculated to be the most stable in **1** and is expected to be maintained in **2**, a large molecular rearrangement is required to achieve the parallel sandwich geometry and the energy barrier needed for excimer formation may be higher than predicted on the basis of the mean distribution of conformers at room temperature.

5. Conclusions

We have quantitatively studied the process of excimer formation by spectroscopy and kinetic analysis in three flexible bisbenzene compounds connected by the O–CH_2–O chain. The experimental results obtained both in solution and in the supersonic jet conditions allow to shed light on the energetics and dynamics of the reaction and to emphasize the following features: (1) The fluorescence emission in the monomer region exhibits a biexponential behavior according to the simple kinetic scheme developed by Birks. The high value of the excimer formation rate ($1–5\times10^{11}$ s^{-1}) is in line with the outstanding flexibility of the acetal link. (2) The temperature dependence of the fluorescence time evolution has been used to extract the thermodynamic parameters in methanol and in methylcyclohexane for **2**. It has been shown that, while the heights of the barrier are very close for both solvents, the preexponential factors in the Arrhenius expression of the excimer formation rate constants are clearly affected by the viscosity of the solvents. (3) The molecular energy barrier for excimer formation in the isolated bichromophore **2** has been estimated to be larger than 2.3 kcal mol^{-1}.

Acknowledgements

We thank Marko Baller for assistance in the measurements and the Region Aquitaine for financial support. We are also greatly indebted to Pr. J. Hynes for stimulating suggestions.

References

[1] J. Ferguson, A. Castellan, J.P. Desvergne, H. Bouas-Laurent, Chem. Phys. Lett. 78 (1981) 446–450.

[2] J. Ferguson, A.W. Mau, Mol. Phys. 27 (1974) 377–387.
[3] H. Bouas-Laurent, J.-P. Desvergne, in: H. Dürr, H. Bouas-Laurent (Eds.), Photochromism. Molecules and Systems, Chap. 14, Elsevier, Amsterdam, 1990.
[4] J. Gallego, F. Mendicuti, E. Saiz, W.L. Mattice, Polymer 34 (1993) 2475–2480.
[5] M. Goldenberg, J. Emert, H. Morawetz, J. Am. Chem. Soc. 100 (1978) 7171–7177.
[6] E. Pajot-Augy, L. Bokobza, L. Monnerie, A. Castellan, H. Bouas-Laurent, Macromolecules 17 (1984) 1490–1496.
[7] F.C. De Schryver, N. Boens, M. Van Der Auweraer, L. Viaene, S. Reekmans, B. Hermans, J. Van Stam, M. Gehlen, H. Berghmans, M. Berghmans, M. Ameloot, Pure Appl. Chem. 67 (1995) 157–165.
[8] K.A. Zachariasse, W. Kühnle, A. Weller, Chem. Phys. Lett. 73 (1980) 6–11.
[9] T. Ikeda, B. Lee, S. Tazuke, A. Takenaka, J. Am. Chem. Soc. 112 (1990) 4650–4656.
[10] A. Castellan, J.P. Desvergne, H. Bouas-Laurent, Chem. Phys. Lett. 76 (1980) 390–397.
[11] K.A. Zachariasse, W. Kühnle, A. Weller, Chem. Phys. Lett. 59 (1978) 375–380.
[12] K.A. Zachariasse, R. Busse, G. Duveneck, W. Kühnle, J. Photochem. 28 (1985) 237–253.
[13] E.A. Chandross, C.J. Dempster, J. Am. Chem. Soc. 92 (1970) 3586–3593.
[14] G.D. Scholes, K.P. Ghiggino, G.J. Wilson, Chem. Phys. 155 (1991) 127–141.
[15] F. Hirayama, J. Chem. Phys. 42 (1965) 3163–3167.
[16] T.A. Smith, D.A. Shipp, G.D. Scholes, K.P. Ghiggino, J. Photochem. Photobiol. A: Chem. 80 (1994) 177–185.
[17] T. Chakraborty, E.K.C. Lim, Phys. Chem. 99 (1995) 17505–17508.
[18] J.P. Desvergne, H. Bouas-Laurent, F. Lahmani, J. Sepiol, J. Phys. Chem. 96 (1992) 10616–10622.
[19] J.P. Desvergne, M. Gotta, J.C. Soulignac, J. Lauret, H. Bouas-Laurent, Tetrahedron Lett. 36 (1995) 1259–1262.
[20] H. Hopf, R.H. Utermöhlen, P.G. Jones, J.P. Desvergne, H. Bouas-Laurent, J. Org. Chem. 57 (1992) 5509–5517.
[21] A. Zehnacker, F. Lahmani, E. Bréhéret, J.P. Desvergne, H. Bouas-Laurent, A. Germain, V. Brenner, P. Millié, Chem. Phys. 208 (1996) 243–257.
[22] E.V. Dehmlov, J. Schmidt, Tetrahedron 32 (1976) 95–99.
[23] I.B. Berlman, in: Handbook of Fluorescence Spectra of Aromatic Molecules, Academic Press, New York, 1965.
[24] T. de Roeck, N. Boens, J. Dockx, DECAN 1.0, K.U. Leuven, Belgium.
[25] J.B. Birks, Photophysics of Aromatic Molecules, Wiley-Interscience, London, 1970, pp. 301–371.
[26] I. Tinoco Jr., J. Am. Chem. Soc. 82 (1960) 4785–4790.
[27] I. Tinoco Jr., J. Am. Chem. Soc. 83 (1961) 5047–5048.
[28] D.T. Browne, J. Eisinger, N.J. Leonard, J. Am. Chem. Soc. 90 (1968) 7302–7323.
[29] B. Stevens, M.I. Ban, Trans. Faraday Soc. 60 (1964) 1515–1523.
[30] S. Yamamoto, K. Okuyama, M. Mikami, M. Ito, Chem. Phys. Lett. 125 (1986) 508–511.
[31] J. Emert, D. Kodali, R. Catena, J. Chem. Soc., Chem. Commun., 1981, 758–759.
[32] J. Emert, P. Phalon, R. Catena, D. Kodali, J. Chem. Soc., Chem. Commun., 1981, 759–760.
[33] S. Hamai, Bull. Chem. Soc. Jpn. 59 (1986) 2979–2982.
[34] F.C. De Schryver, K. Demeyer, J. Heybrechts, H. Bouas-Laurent, A. Castellan, J. Photochem. 20 (1982) 341–354.
[35] J.P. Desvergne, N. Bitit, A. Castellan, H. Bouas-Laurent, J.C. Soulignac, J. Lumin. 37 (1987) 175–181.
[36] H.A. Kramers, Physica (Utrecht) 7 (1940) 284.
[37] J.A. Riddick, W.B. Bunger in: Organic Solvents, Techniques of Chemistry, Wiley-Interscience, New York, 1970.